

Prognostic biomarker CPEB3 and its associations with immune infiltration in clear cell renal cell carcinoma

HUALAN HONG^{1,2}, XI SHI^{1,2}, WENYONG OU³ and PENGJU OU^{1,4}

¹Department of Medical Oncology, Cancer Center, The First Affiliated Hospital of Fujian Medical University;

²Department of Medical Oncology, National Regional Medical Center, Binhai Campus of The First Affiliated Hospital of Fujian Medical University, Fuzhou, Fujian 350000; ³Department of Surgery 1, Longyan People Hospital, Longyan, Fujian 364000;

⁴Department of Medical Affairs, Guangzhou Lupeng Pharmaceutical Co., Ltd. Guangzhou, Guangdong 510000, P.R. China

Received September 1, 2023; Accepted January 17, 2024

DOI: 10.3892/br.2024.1751

Abstract. The role and underlying mechanism of cytoplasmic polyadenylation element binding protein 3 (CPEB3) in clear cell renal cell carcinoma [ccRCC progression remain poorly characterized. The present study was designed to evaluate the role of CPEB3 in ccRCC and its clinical associations. The overall response rate of first-line therapies (ICIs combined with VEGFR-TKIs or ICI combination) for ccRCC] is 42.0-59.3%, so a number of patients with ccRCC do not benefit from these therapies. To avoid immunosurveillance and immune killing, tumor cells decrease immunogenicity and recruit immunosuppressive cells such as regulatory T cells (Tregs). Tregs inhibit the development of anti-tumor immunity, thereby hindering immune surveillance of cancer and preventing effective anti-tumor immune response in tumor-bearing hosts. The present study analyzed clinical specimens from patients ccRCC and then examined the role of CPEB3 in ccRCC via bioinformatics analysis. CPEB3 expression was significantly reduced in ccRCC compared with normal tissue and low CPEB3 expression was associated with poor overall survival. Moreover, CPEB3 expression was an independent predictor of survival. CPEB3 expression was positively associated with immune biomarkers [CD274, programmed cell death 1 ligand 2, Hepatitis a virus cellular receptor 2, Chemokine (C-X-C motif) ligand (CXCL)9, CXCL10, Inducible T cell costimulatory, CD40, CD80 and CD38] that improve the outcome of anti-tumor immune responses. CPEB3 expression in ccRCC also affected the status of 24 types of infiltrating immune cell, of which Tregs were the most significantly negatively correlated cell type. CPEB3 may serve as a prognostic

biomarker in ccRCC and its mechanism may be related to the regulation of Tregs.

Introduction

The incidence of renal cell carcinoma (RCC) has increased in past decades: RCC accounts for 2-3% of adult malignancies worldwide and is the 14th most common type of solid cancer, with 431,288 new cases reported in 2020 (1). The dominant subtype is clear cell (cc)RCC (2). Immune checkpoint inhibitors (ICIs) that target programmed death receptor-1 (PD-1) on T cells have been widely used to treat advanced renal cancer (3-11). Tyrosine kinase inhibitors of vascular endothelial growth factors combined with ICIs have been approved as first- and subsequent-line therapies for advanced ccRCC (3-8). ICI combination (9) is recommended as first- and subsequent-line therapy for advanced ccRCC and ICI monotherapy (10) has been recommended as subsequent-line therapy by The National Comprehensive Cancer Network. In addition, ICIs have been investigated as adjuvant therapy options for ccRCC with positive results (11). The overall response rate of first-line therapies is 42.0-59.3% (5,7-9). Although the overall response rate is higher than that of traditional options, such as chemotherapy or radiotherapy, numerous patients do not benefit from these therapies. Therefore, screening of the targeted population and detection of ICI resistance is key.

The tumor microenvironment (TME) is associated with poor prognosis in patients with numerous types of cancer [renal cell carcinoma (12), non-small cell lung cancer (13), Liver Cancer (14), and so on]. TME involves the recruitment of immunosuppressive cells, such as regulatory T (Treg) and myeloid-derived suppressor cells and tumor-associated macrophages (15-18). Multiple mechanisms of Treg-mediated immunosuppression have been described, including cell contact-dependent and humoral factor-mediated mechanisms, that involve a range of molecules, such as cell surface molecules [programmed death (PD)-1, Programmed death-ligand 1(PD-L1), Cytotoxic T-lymphocyte-associated antigen 4 (CTLA-4), CD25, T cell immunoreceptor with Ig and ITIM domains (TIGIT), CD39 and CD73], cytokines (IL-2, IL-10, TGF- β and IL-35) and secreted or intracellular molecules (granzyme, cyclic AMP and Indoleamine 2,3-dioxygenase)] (19).

Correspondence to: Dr Pengju Ou, Department of Medical Affairs, Guangzhou Lupeng Pharmaceutical Co., Ltd., Guangzhou, Suite 801, 60 Science Avenue, Huangpu, Guangzhou, Guangdong 510000, P.R. China
E-mail: oupj3@mail3.sysu.edu.cn

Key words: cytoplasmic polyadenylation element binding protein 3, clear cell renal cell carcinoma, regulatory T cell, immune infiltration, survival analysis

Tregs are a highly immunosuppressive subset of CD4⁺ T cells that are distinguished from other immune cells by expression of forkhead box protein 3 (FoxP3) transcription factor. Tregs maintain immune homeostasis by controlling immune responses and are associated with several diseases, including autoimmune diseases and cancer (20-23). Tumors are infiltrated by multiple Tregs, which account for 10-50% of CD4⁺ T cells in tumors and 2-5% of CD4⁺ T cells in the peripheral blood of those without cancer (24-26).

Cytoplasmic polyadenylation element binding protein 3 (CPEB3), a member of the CPEB family (27), has a tumor-suppressive effect in numerous types of cancers, such as gastric cancer (28) and esophageal squamous cell carcinoma (29). Particularly in colorectal cancer, CPEB3 is involved in cross-talk between colorectal cancer cells and tumor-associated macrophages by targeting IL-6 receptor/STAT3 signaling (30). However, the exact role and underlying mechanism of CPEB3 in ccRCC progression remain poorly characterized. The present study examined the expression of CPEB3 in ccRCC tissue to provide insights into the inhibition of Treg infiltration in TME.

Materials and methods

Clinical specimens. ccRCC tissue microarrays (TMAs; HKIdE180Su03) were obtained from Shanghai Xinchao Biological Technology Co. Ltd. HKIdE180Su03 contains 90 pairs of ccRCC and matched paracancerous tissue that were used for immunohistochemistry (IHC) analysis. Outdo BioTech also provided the detailed clinicopathological characteristics of cohorts. The Clinical Research Ethics Committee of Outdo BioTech granted ethical approval for the study of the TMAs (Shanghai, China; approval no. SHYJS-CP-1707003).

IHC. IHC staining was performed on TAMs to detect protein expression levels of CPEB3. In brief, tissue samples were fixed in 4% paraformaldehyde for 8 h at room temperature, then embedded in paraffin and sliced into 3- μ m thick sections. Sections were deparaffinized with xylene at room temperature for 30 min and rehydrated using a descending ethanol series. Sections were heated in a water bath at 95°C with Dako Target Retrieval Solution (Code S1699; Agilent Technologies, Inc.) for 20 min. Sections were then treated with 3% hydrogen peroxide in methanol to quench the endogenous peroxidase activity, followed by incubation with normal goat serum (10%; Beijing Biosynthesis Biotechnology Co., Ltd.) for 10 min at room temperature to block the nonspecific binding. Sections were incubated with rabbit polyclonal CPEB3 antibody (1:100; cat. no. ab10883; Abcam) for overnight at 4°C, followed by application of a secondary antibody [1:1,000; Peroxidase AffiniPure Goat Anti-Rabbit IgG (H+L); cat. no. 111-035-003; Jackson ImmunoResearch Laboratories, Inc.] for 40 min at 37°C. DAB was used as the chromogenic substrate and the sections were counterstained with hematoxylin for 1 min at 20°C. Positive controls were performed in each experiment. Negative controls were performed in the same condition without primary antibodies. Full slide images were reviewed and evaluated by two pathologists under a light microscope (Aperio XT; Leica biosystems; magnification, x40).

Immunostaining intensity ranged from weak to strong as follows: 0, no staining; 1 (weak staining), 2 (low to moderate staining), 3 (moderate staining) or 4, strong staining). The final score was calculated as proportion of CPEB3-positive cells multiplied by staining intensity. Tumors were divided in high- or low-expression groups based on a final score ≥ 300 or < 300 , respectively. Each sample was independently assessed by two experienced pathologists, with a third pathologist making the final decision in case of disagreement.

Data collection and processing. University of California, Santa Cruz XENA (31) (xenabrowser.net/datapages/) runs Toil (32) to capture and process data from The Cancer Genome Atlas (33) and the Genotype Tissue Expression Project (34). Toil was used to collect data from normal and diseased tissue of patients with pan-cancer and ccRCC for statistical analyses and visualization using the R programming language (version 4.2.1) (35). RNA sequencing data were converted into the transcripts per million reads format.

Analysis of expression levels of CPEB3 and co-expressed and differentially expressed genes. Expression levels of CPEB3 were compared between normal and tumor tissues using the Stat package (version 4.2.1) (<https://www.r-project.org/>). Total protein expression of CPEB3 and its methylation levels in ccRCC were also identified using the UALCAN database (36,37). The Stat package was used to identify co-expressed genes. Furthermore, after dividing the samples into groups based on the median expression of CPEB3 (cut-off value, 2.2454), differentially expressed genes were identified using DESeq2 (version 1.36.0) (38) with the following threshold parameters: Log-fold change absolute value > 1.5 and $P < 0.05$. The results were visualized using ggplot2 package (version 3.3.6) (39).

Analysis of biological function. Gene Ontology (GO) (40,41) and Kyoto Encyclopedia of Genes and Genomes (KEGG; kegg.jp) pathways were used to determine the biological functions of CPEB3 in ccRCC. The three primary components in GO analysis are molecular function (MF), biological process (BP) and cellular component (CC). These analyses were performed using clusterProfiler (version 4.4.4) (42) and Gplot (version 1.0.2) packages (43). Gene Set Enrichment Analysis (GSEA) (44) was performed to explore underlying functions and pathways in the Human Molecular Signatures Database collections (c2.cp.all.v2022.1.Hs.symbols.gmt) (45).

Analysis of CPEB3-associated immune cell infiltration and correlation with immune checkpoints and cell markers. To detect whether CPEB3 expression influences immune cell infiltration, status of 24 types of infiltrating immune cells (46) in ccRCC was determined using the gene set variation analysis package (version 1.46.0) (47). Tumor Immune System Interaction database was used to determine the relationship between abundance of tumor-infiltrating lymphocytes and expression of CPEB3. The immune-associated signatures of tumor-infiltrating lymphocytes were obtained from the study by Charoentong *et al.* (48). Association between Tregs and CPEB3 was assessed using TIMER2.0 (timer.cistrome.org/) (49). Associations between CPEB3 and immune checkpoints [including CD274, B and T lymphocyte attenuator,

lymphocyte-activation gene3 (LAG3) and CTLA] cell markers (such as FOXP3) were analyzed using the ggplot2 package.

Clinical significance of CPEB3 in ccRCC. CPEB3 expression and OS was analyzed by Kaplan-Meier survival curves, a log-rank test and univariate and multivariate Cox regression models. Survival package (version 3.3.1) (50) was used for subgroup analysis and forest plots were constructed using ggplot2. Survival package was used to generate the Kaplan-Meier overall survival (OS) and disease-specific survival (DSS) curves for ccRCC. Associations between CPEB3 expression and clinical features were assessed using ggplot2. Receiver operating characteristic (ROC) curves were constructed using the pROC package (version 1.18.0.) (51) to determine whether CPEB3 could be a tumor prediction index. Rms (version 6.3.0; cran.r-project.org/web/packages/rms/index.html) and survival packages were used to construct the nomogram.

Statistical analysis. Mann-Whitney U test was used to compare the difference in expression of CPEB3 between normal tissue and tumors in pan-cancer. The significance of clinicopathological variables for survival was analyzed using the univariate and multivariate Cox proportional hazards method. The Mann-Whitney U test was also used to compare expression of CPEB3 in immune cells. Paired t test was used to analyze the expression of CPEB3 in paired samples of ccRCC. The chi-square test was used for comparisons of CPEB3 expression in clinicopathological features. Data are presented as the mean \pm SEM. Hypergeometric distribution test was used for GO/KEGG analysis. Permutation test calculated the likelihood of occurrence of the observed enrichment score (ES). Cox regression analysis and Kaplan-Meier method with long-rank test were used for prognostic analysis of CPEB3. The Shapiro-Wilk normality test was performed to evaluate the normality and then Pearson or Spearman correlation was utilized to calculate correlation coefficients. All statistical analyses of bioinformatics data were performed using R programming language. $P < 0.05$ was considered to indicate a statistically significant difference.

Results

Clinicopathological features of study population. The main clinicopathological features of the ccRCC series are summarized in Table I. Male patients outnumbered female (59:30) patients and the median patient age was 59 years (range, 29-82 years; data not shown). All patients were Asian, 90.8% presented with localized disease (stages I and II) and 9.2% presented with advanced disease (stages III and IV) according to American Joint Committee on Cancer Cancer Staging Manual (52) at the time of diagnosis and received systemic therapy (data not shown). The median tumor size was 4.5 cm (data not shown) with 23.3% of tumors measuring >7 cm. Overall, 64.4% of ccRCCs were T1, 28.9% T2 and 6.7% T3. Additionally, 97.7% of the patients were pN0 and 2.3% were pN1. The percentage of patients with distant metastases was 2.2% (Data not shown). Moreover, 63.2% of the tumors were stage I, 27.6% were stage II, 6.9% were stage III, and 2.3% were stage IV; 30% of ccRCCs were grade 1, 46.7% were grade 2, 23.3% were grade 3 and 0.0% were grade 4 (53).

Table I. Patient clinicopathological features.

Characteristic	Number (%)
Age, years	
≤ 60	50 (56.8)
> 60	38 (43.2)
Sex	
Male	59 (66.3)
Female	30 (33.7)
T stage	
T1	58 (64.4)
T2/3	32 (35.6)
N stage	
N0	85 (97.7)
N1	2 (2.3)
M stage	
M0	88 (97.8)
M1	2 (2.2)
TNM stage	
I	55 (63.2)
II	24 (27.6)
III	6 (6.9)
IV	2 (2.3)
Furhman grade	
1	27 (30.0)
2	42 (46.7)
3	21 (23.3)
4	0 (0.0)
Maximum tumor diameter, cm	
≤ 7	69 (76.7)
> 7	21 (23.3)

Some baseline data were missing due to loss of follow-up.

CPEB3 expression is depressed in ccRCC tissue. CPEB3 expression was examined using IHC in 81 pairs of human ccRCC and adjacent non-cancerous tissue samples (Fig. 1A). CPEB3 staining was observed only in the cytoplasm of the cells. High CPEB3 expression was observed in 96.3% (78/81) of normal renal and 30.9% (25/81) of the ccRCC tissue samples (Fig. 1B). ccRCC expression was not associated with sex, age, distant metastasis, tumor stage, histological grade or lymph node metastasis (Table SI).

Prognostic value of CPEB3 expression in patients with ccRCC. To determine the prognostic value of CPEB3 expression, association between CPEB3 expression and OS was analyzed by Kaplan-Meier survival curves, a log-rank test and univariate and multivariate Cox regression models. The median follow-up time was 93 months (range, 2-106 months), and 64.4% of the patients were alive without evidence of disease. Compared with high CPEB3 expression, low expression was associated with shorter OS (Fig. 1C). To identify the clinicopathological variables associated with survival

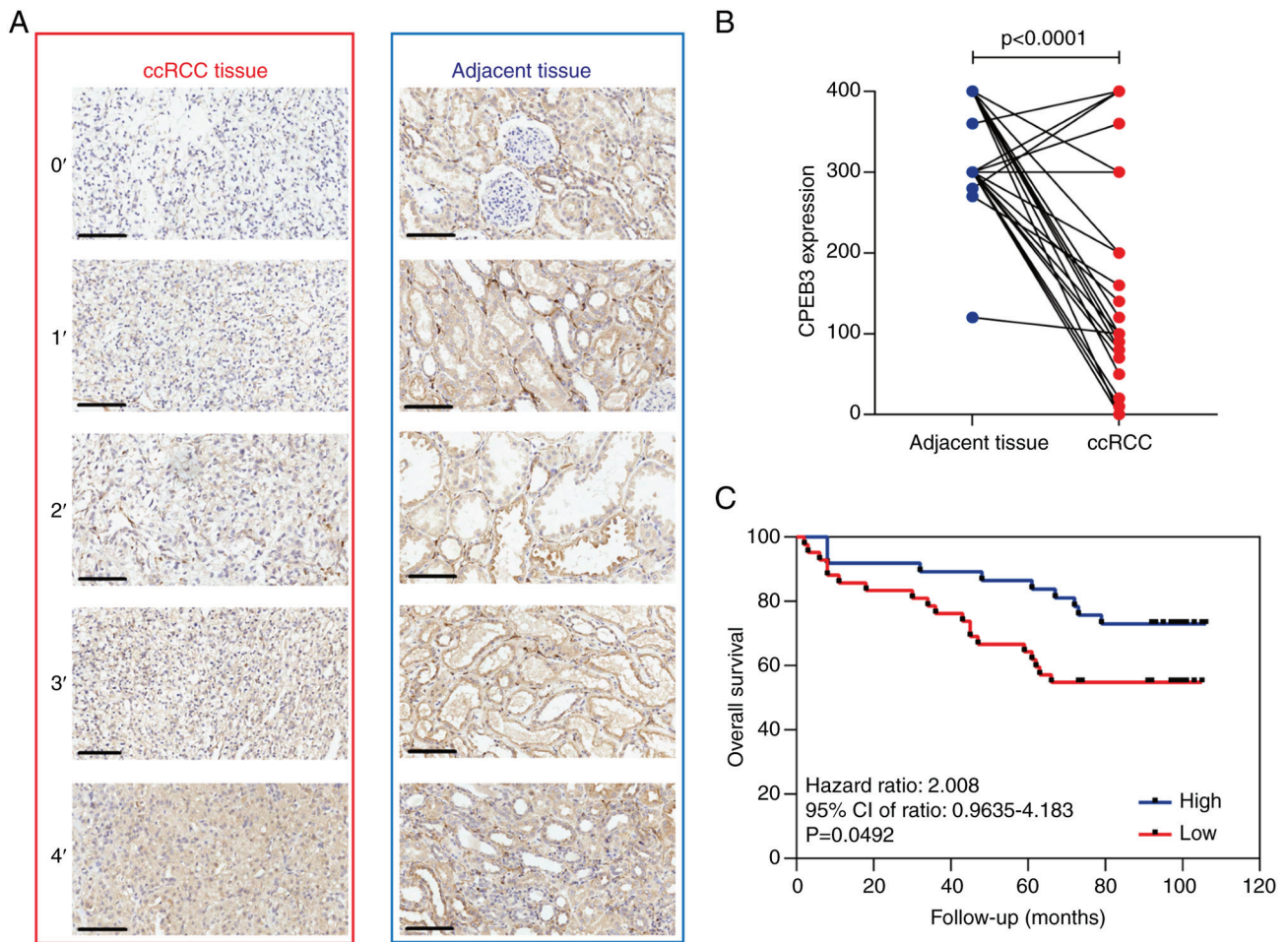


Figure 1. CPEB3 expression and overall survival. (A) Protein expression of CPEB3 in ccRCC and corresponding adjacent non-cancerous tissue were detected by immunohistochemistry staining. Immunostaining intensity was scored as follows: 0': no staining; 1': weak staining; 2': low to moderate staining; 3': moderate staining; 4': strong staining. Scale bar, 100 μ m. (B) Expression of CPEB3 in 81 pairs of ccRCC and adjacent non-cancerous tissue samples. (C) Overall survival in patients with high or low CPEB3 expression. CPEB3, cytoplasmic polyadenylation element binding protein 3; ccRCC, clear cell renal cell carcinoma.

time, univariate analysis (sex, age, tumor size, T, N and M stage, tumor grade and CPEB3 expression) was performed. Differences in prognosis were expressed as hazard ratios (HR) and P-values. Univariate analysis demonstrated that age, tumor size, T, N and M stage, tumor grade and CPEB3 expression were significant predictors of OS (Table II). The relative importance of each variable was determined using multivariate Cox proportional hazards analysis. Multivariate analysis showed that age, T and N stage and CPEB3 expression were independent predictors of OS. Patients with low CPEB3 expression had a 3.57-time higher risk of death than those with high expression (HR, 0.28, 95% CI, 0.091-0.865; Table II).

Expression of CPEB3 in pan-cancer and ccRCC. Expression levels of CPEB3 were assessed in 33 cancer types (Fig. 2A); compared with normal tissues, 16 cancer types expressed lower levels of CPEB3. The expression of CPEB3 in ccRCC tissues was significantly lower than that in normal tissue (Fig. 2B) and total protein expression of CPEB3 was also lower in ccRCC samples compared with normal tissue (Fig. 2C). Additionally, the methylation of CPEB3 in ccRCC was higher than that in normal tissue (Fig. 2D).

Differentially and co-expressed genes of CPEB3. By setting the threshold of absolute log fold-change to >1.5 and P-value <0.05 , 897 genes were identified as differentially expressed; 652 of these were downregulated and 245 were upregulated (Fig. 2E). The top 15 differentially and 50 co-expressed genes (most significant) are presented in a heat map (Fig. 2F and G).

Biological functions and associated pathways of CPEB3. Biological functions and related pathways of CPEB3 were investigated by GO and KEGG analysis of differentially expressed genes (Fig. 3A; Table SII). BPs included 'acute-phase response', 'humoral immune response' and 'acute inflammatory response'; CCs included 'blood microparticle', 'immunoglobulin complex' and 'high-density lipoprotein particle'; MFs included 'structural constituent of skin epidermis', 'serine-type endopeptidase activity' and 'serine-type peptidase activity'. A total of three KEGG pathways were enriched: 'Complement and coagulation cascades', 'fat digestion and absorption' and 'collecting duct acid secretion'. GSEA was used to explore the possible mechanisms affected by CPEB3 (Fig. 3B). The differentially expressed genes were associated with ROSTY

Table II. Univariate and multivariate Cox proportional hazards model for overall survival in patients with clear cell renal cell carcinoma.

Characteristic	n	Univariate analysis		Multivariate analysis	
		Hazard ratio (95% CI)	P-value	Hazard ratio (95% CI)	P-value
Sex			0.994		
Female	30	Reference			
Male	59	1.003 (0.466-2.157)	0.994		
Age	88	1.056 (1.019-1.094)	0.003 ^a	1.090 (1.040-1.142)	<0.001 ^a
T stage			<0.001 ^a		
T2	26	Reference		Reference	
T1	58	0.278 (0.126-0.612)	0.002 ^a	0.312 (0.121-0.807)	0.016 ^a
T3	6	1.952 (0.640-5.953)	0.240	2.912 (0.559-15.179)	0.205
N stage			0.009 ^a		
N0	85	Reference		Reference	
N1	2	16.403 (3.288-81.826)	<0.001 ^a	6.134 (1.090-34.530)	0.040 ^a
M stage			0.019 ^a		
M0	88	Reference		Reference	
M1	2	10.477 (2.307-47.585)	0.002 ^a	1.177 (0.135-10.282)	0.883
Tumor size	90	1.208 (1.077-1.356)	0.001 ^a	1.144 (0.981-1.335)	0.087
CPEB3 expression			0.027 ^a		
Low	59	Reference		Reference	
High	26	0.343 (0.119-0.993)	0.048 ^a	0.280 (0.091-0.865)	0.027 ^a

^aP<0.05. CPEB3, cytoplasmic polyadenylation element binding protein 3.

Cervical Cancer Proliferation Cluster, SOTIRIOUS Breast Cancer Grade 1 vs. 3 Up, MORI Immature B Lymphocyte Dn, MORI Large Pre Bii Lymphocyte Up, LEE Early T Lymphocyte Up, KOBAYASHI EGFR Signaling 24 h Dn, SHEDDEN Lung Cancer Poor Survival A6, HOFFMANN Large To Small Pre Bii Lymphocyte Up, MORI Mature B Lymphocyte Dn, FISCHER G2/M Cell Cycle, [Reactome] DNA replication, MANALO Hypoxia Dn, GOBERT Oligodendrocyte Differentiation Up, [Reactome] Cell Cycle Checkpoints, TARTE Plasma Cell vs. Plasmablast Dn, GOLDRATH Antigen Response, MARKEY RB1 Acute Lof Up, PUJANA BRCA2 Pcc Network, [Reactome] Cell Cycle Mitotic, [Reactome] M Phase, HELLER Silenced By Methylation Up.

Association between CPEB3 expression and infiltrating immune cells. A total of 24 types of infiltrating immune cells influenced by CPEB3 expression in ccRCC were assessed (Fig. 4A). Among all cell types, negatively correlated infiltrating immune cells were activated DC, B, cytotoxic, natural killer CD56^{bright} cell, T helper (Th)1 and 2 cells and Tregs (Fig. 4B). Positively correlated infiltrating immune cells were eosinophils, mast and Th cells, T central memory (Tcm), T effector memory (Tem), T $\gamma\delta$ and Th17 cells (Fig. 4C). Tregs were the most significantly negatively correlated infiltrating immune cells, whereas Tcm was the most significantly positively correlated type. Tregs were further confirmed to be significantly negatively correlated

with CPEB3 expression in ccRCC using TIMER2.0 and TISIDB (Fig. 4D and E). CPEB3 expression was positively correlated with immune biomarkers CD274, programmed cell death 1 ligand 2 (PDCD1LG2), Hepatitis a virus cellular receptor 2 (HAVCR2), Chemokine (C-X-C motif) ligand (CXCL)9, CXCL10, Inducible T cell costimulatory (ICOS), CD40, CD80 and CD38 (Fig. 5A). CPEB3 expression was inversely associated with immune biomarkers FOXP3, LAG3 and Nuclear receptor subfamily 2, group F, member 6 (NR2F6) (Fig. 5B).

Clinical implications of CPEB3 expression in ccRCC. Patients with ccRCC with different characteristics, such as sex, age, grade and T, N and M stages, were grouped according to expression of CPEB3. Patients with high CPEB3 expression showed better OS regardless of sex and age (Fig. 6A). High CPEB3 expression in patients with grade 1 and 2, T stage 1 and 2, N0 and M0 was associated with favorable survival (Fig. 6A). Moreover, CPEB3 expression levels were significantly associated with prognosis of patients with ccRCC. Kaplan-Meier curves showed that patients with high CPEB3 expression had better OS and DSS (Fig. 6B). These patients also had better clinical features, such as tumor grade and T, M and pathological stage (Fig. 6C). The ROC curve analysis indicated that the area under the curve for ccRCC was 0.916 (Fig. 6D). Finally, the constructed nomogram could be used as a powerful tool to predict survival probability at 1, 3 and 5 years (Fig. 6E).

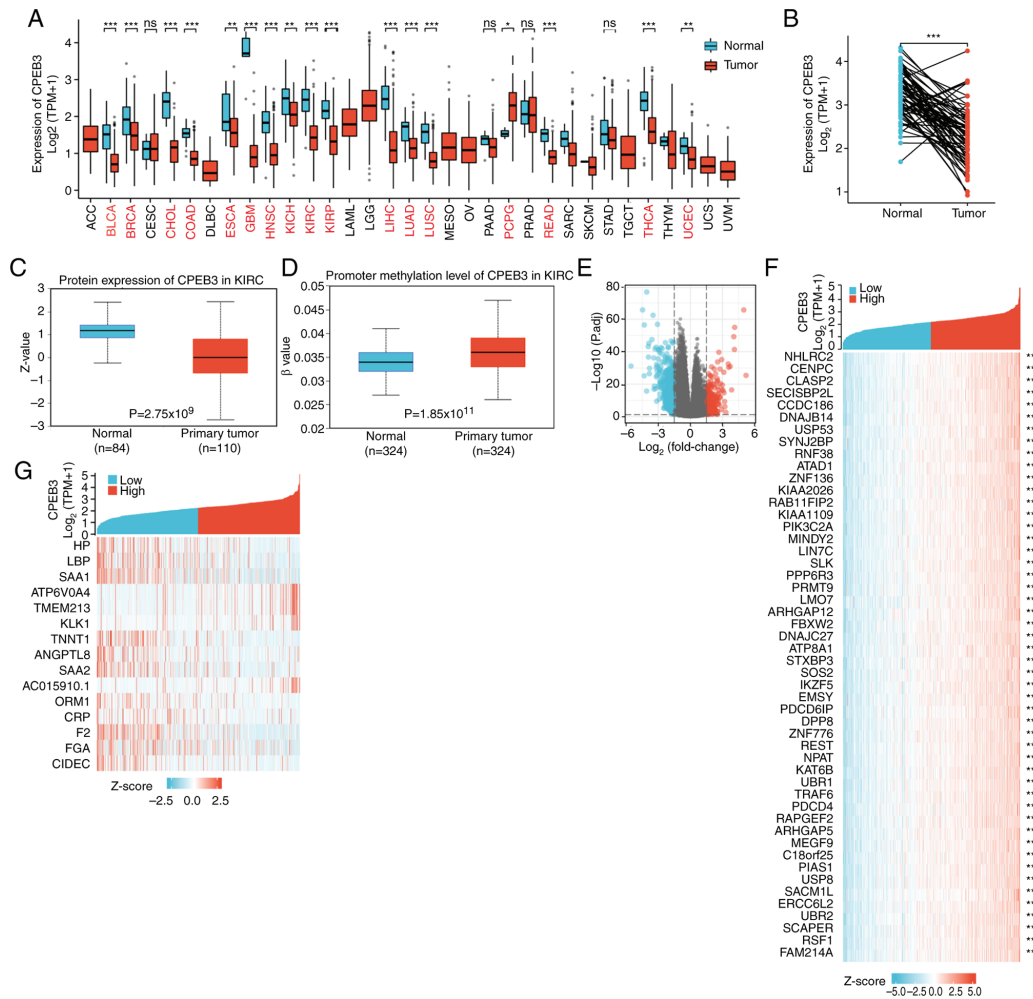


Figure 2. Expression levels of CPEB3 and differentially expressed genes and co-expressed genes. (A) CPEB3 expression levels in 33 types of cancer and corresponding adjacent normal tissue. Red, tumors with significant differences in CPEB3 expression compared with normal tissue. (B) Expression of CPEB3 [paired samples (n=72)] in ccRCC. (C) Protein expression of CPBE3 in ccRCC. (D) Methylation of CPEB3 in ccRCC. (E) Volcano plot and (F) heat map differentially expressed genes. Error bars indicate SEM. (G) Co-expressed genes as a heap map. *P<0.05, **P<0.01, ***P<0.001 vs. normal. CPEB3, cytoplasmic polyadenylation element binding protein 3; ccRCC, clear cell renal cell carcinoma; KIRC, kidney renal clear cell carcinoma; TPM, transcript per kilobase per million mapped reads; ns, no significance.

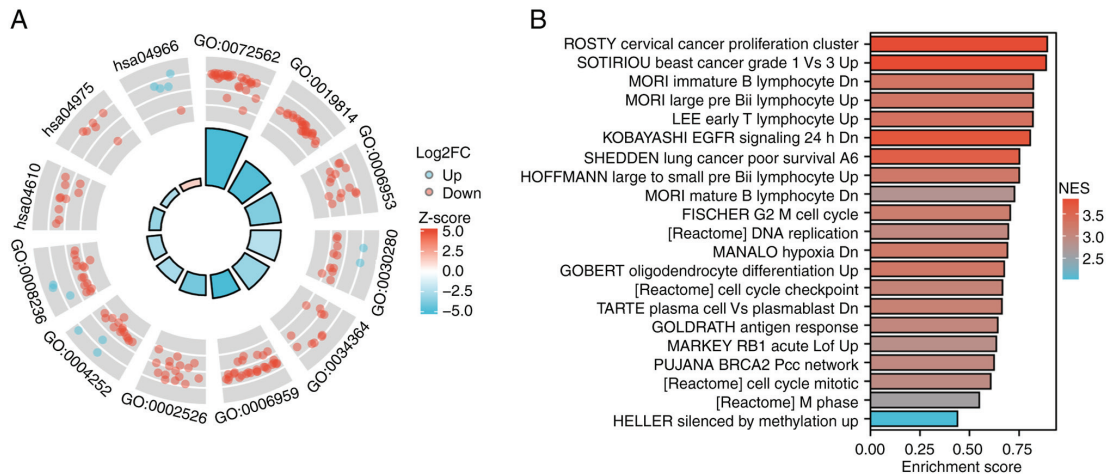


Figure 3. Functional enrichment analysis of differentially expressed genes based on CPEB3 expression in clear cell renal cell carcinoma. (A) Enriched biological functions (GO:0006953/acute-phage response, GO:0006959/humoral immune response, GO:0002526/acute inflammatory response), cellular components (GO:0072562/blood microparticle, GO:0019814/immunoglobulin complex, GO:0034364/high-density lipoprotein particle), and molecular functions (GO:0030280/structural constituent of skin epidermis, GO:0004252/serine-type endopeptidase activity, GO:0008236/serine-type peptidase activity) and Kyoto Encyclopedia of Genes and Genomes (hsa04975/fat digestion and absorption, hsa04966/collecting duct acid secretion) enrichment of CPEB3. (B) Gene Set Enrichment Analysis based on the differentially expressed genes between the high and low CPEB3 expression groups. CPEB3, cytoplasmic polyadenylation element binding protein 3; GO, gene ontology; NES, normalized enrichment score.

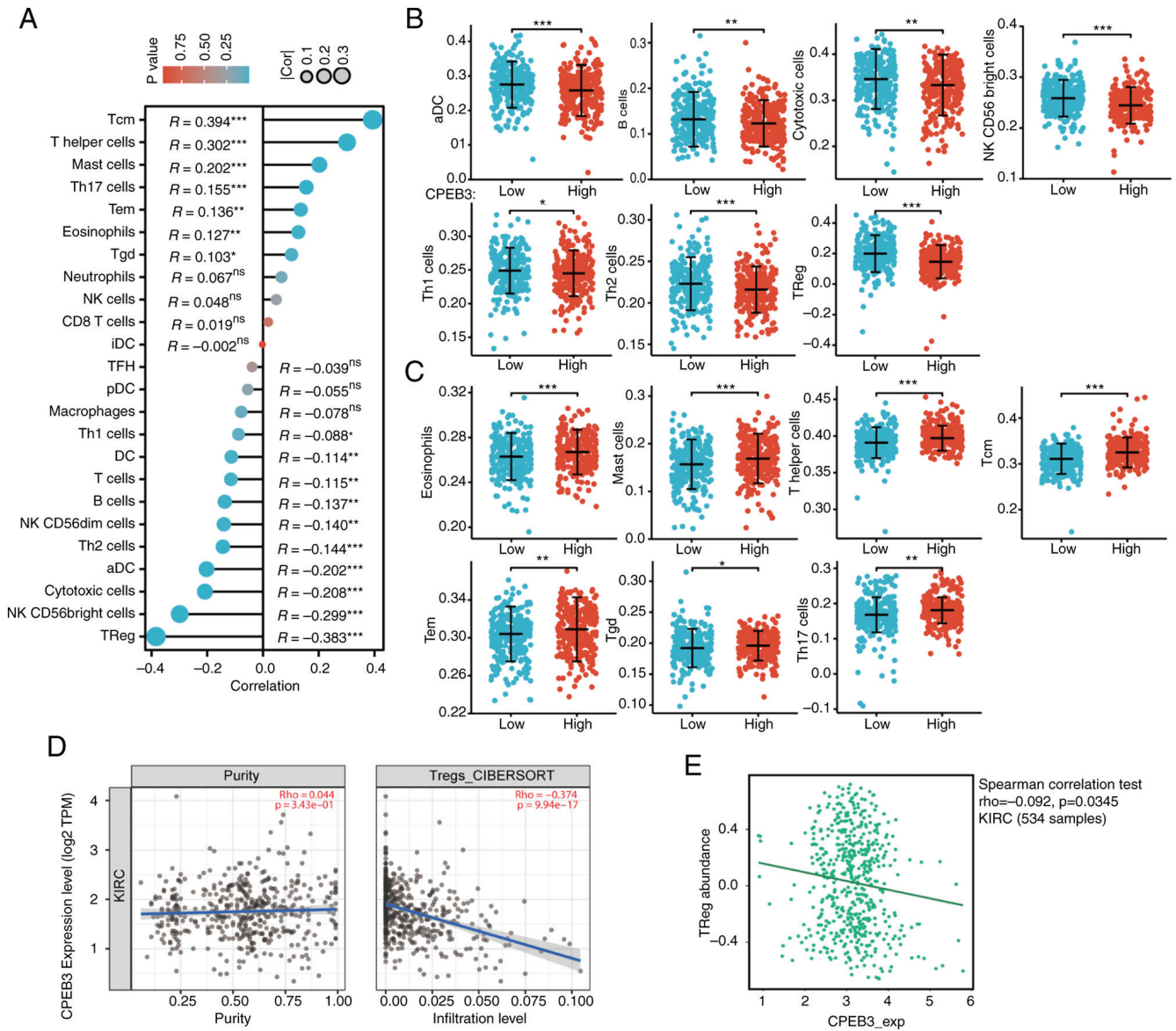


Figure 4. Association between CPEB3 and infiltrating immune cells. (A) Correlation between infiltration levels of 24 immune cell types and CPEB3 expression levels in ccRCC. (B) Negatively and (C) positively correlated infiltrating immune cells. Low CPEB3, n=270; high CPEB3, n=271. Error bars indicate SEM. (D) Association between Tregs and CPEB3 in KIRC samples analyzed by TIMER2.0. (E) Association between Tregs and CPEB3 in 534 KIRC samples analyzed by tumor-immune system interactions database). *P<0.05; **P<0.01 and ***P<0.001. CPEB3, cytoplasmic polyadenylation element binding protein 3; Treg, regulatory T; KIRC, kidney renal clear cell carcinoma; Tcm, T central memory; Th, T helper; Tgd, T gamma delta; NK, natural killer cell; iDC, immature dendritic cell; TFH, T follicular helper; pDC, plasmacytoid dendritic cell; aDC, activated dendritic cell; cor, correlation; TPM, transcript per kilobase per million mapped reads.

Discussion

Timely detection, early intervention and precise therapy have been extensively studied to improve outcomes in patients with ccRCC (54-57). However, these efforts are yet to yield a comprehensive cure. The present study demonstrated decreased CPEB3 protein expression in ccRCC. Furthermore, high CPEB3 expression was associated with a favorable prognosis and was an independent predictor of OS in ccRCC. Nevertheless, ccRCC tissue specimens primarily originated from patients at initial stages of the disease and additional samples, particularly from advanced tumor stages, are required for further studies. Additionally, the molecular mechanisms responsible for CPEB3 expression in cancer

necessitate further investigation. The present study examined the role of CPEB3 in ccRCC via bioinformatics analysis, which revealed low expression of CPEB3 in ccRCC, whereas promoter methylation of CPEB3 was higher in ccRCC than in normal tissue. These results suggest that CPEB3 may act as an important tumor suppressor gene in ccRCC and DNA methylation silences the tumor suppressor function of CPEB3. Patients with high CPEB3 expression had better clinical features and longer survival. ROC curves demonstrated that CPEB3 levels could predict ccRCC with high accuracy. This may support the use of this gene for tumor diagnosis and prognosis in future. However, the present data were retrospective or sourced from a publicly accessible database, which is limited by its retrospective nature. Future investigations should encompass a larger

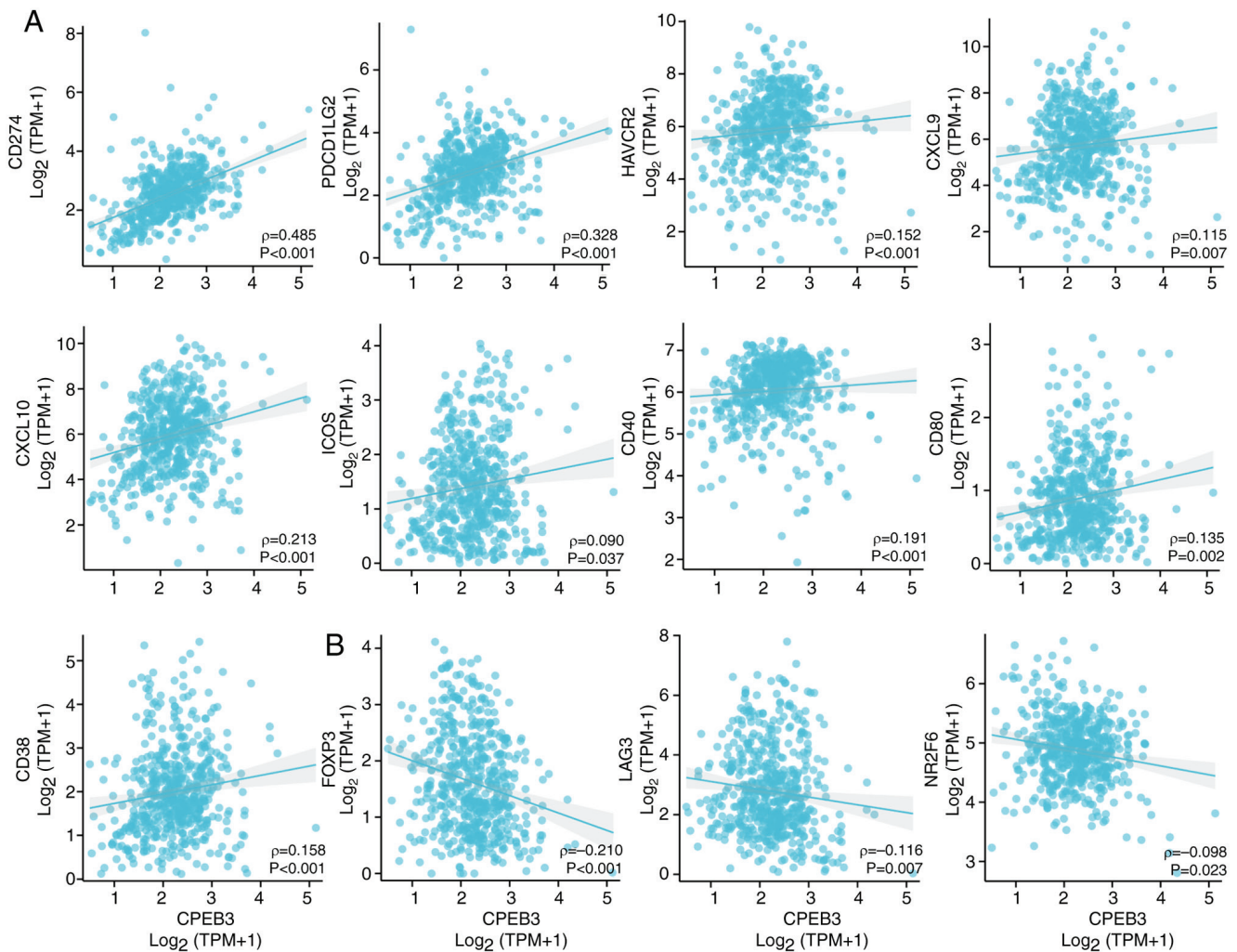


Figure 5. Association between CPEB3 and immune biomarkers. (A) Positively and (B) negatively correlated immune biomarkers. CPEB3, cytoplasmic polyadenylation element binding protein 3; PDCD1LG2, programmed cell death 1 ligand 2; HAVCR2, hepatitis a virus cellular receptor 2; CXCL, Chemokine (C-X-C motif) ligand; ICOS, inducible T cell costimulator; LAG3, lymphocyte activating 3; NR2F6, nuclear receptor subfamily 2 group F member 6; TPM, transcript per kilobase per million mapped reads.

dataset and employ prospective study designs to validate the present findings.

CPEB3 and differentially expressed genes were strongly associated with immune and inflammatory responses. GSEA revealed that CPEB3 may be associated with the immune system, cancer proliferation, differentiation and the cell cycle. These results suggest that CPEB3 may participate in multiple mechanisms of tumor progression.

The immune system serves a leading role in tumor initiation and development (58-63) and ICIs have achieved breakthrough efficacy in the treatment of numerous types of cancer (64-68). Of mechanisms that promote tumor development and ICI responses, those associated with TME are key (69-74). Immune cell infiltrates function as prognostic markers and potential therapeutic targets (75). Cancer-associated fibroblasts (70,76,77), immune cells (76,78) and the extracellular matrix (79) form the TME. Tregs inhibit development of anti-tumor immunity, hinder immune surveillance of cancer and prevent effective anti-tumor immune responses in tumor-bearing hosts. To maintain immune homeostasis, Tregs and effector T cells must be balanced. Here, CPEB3 was

negatively correlated with Tregs, suggesting tumor suppression and enhanced anti-tumor immune effects in ccRCC by promoting CPEB3 expression. However, more experiments are needed to confirm the regulatory effect of CPEB3 on Tregs, such as gene knockout models, and further clarify the mechanism of the interaction between CPEB3 and Treg. In addition, immune biomarkers have been used to predict responses to immunotherapy. CD274 (80), PDCD1LG2 (81), HAVCR2 (82,83), CXCL9 (84), CXCL10 (84), ICOS (85), CD40 (86), CD80 (87) and CD38 (88) have been confirmed to enhance anti-tumor immune responses. FOXP3 (89), LAG3 (90) and NR2F6 (91) are negative regulators of immunotherapy. In the present study, CPEB3 was positively associated with the aforementioned positive genes and negatively associated with negative genes, indicating that CPEB3 may serve as a meaningful biomarker to predict positive immunotherapy responses.

Taken together, the present results showed that CPEB3 may be a tumor suppressor and mediate immune processes in ccRCC. Although these results were based on a retrospective analysis of clinical data and public databases, they provide

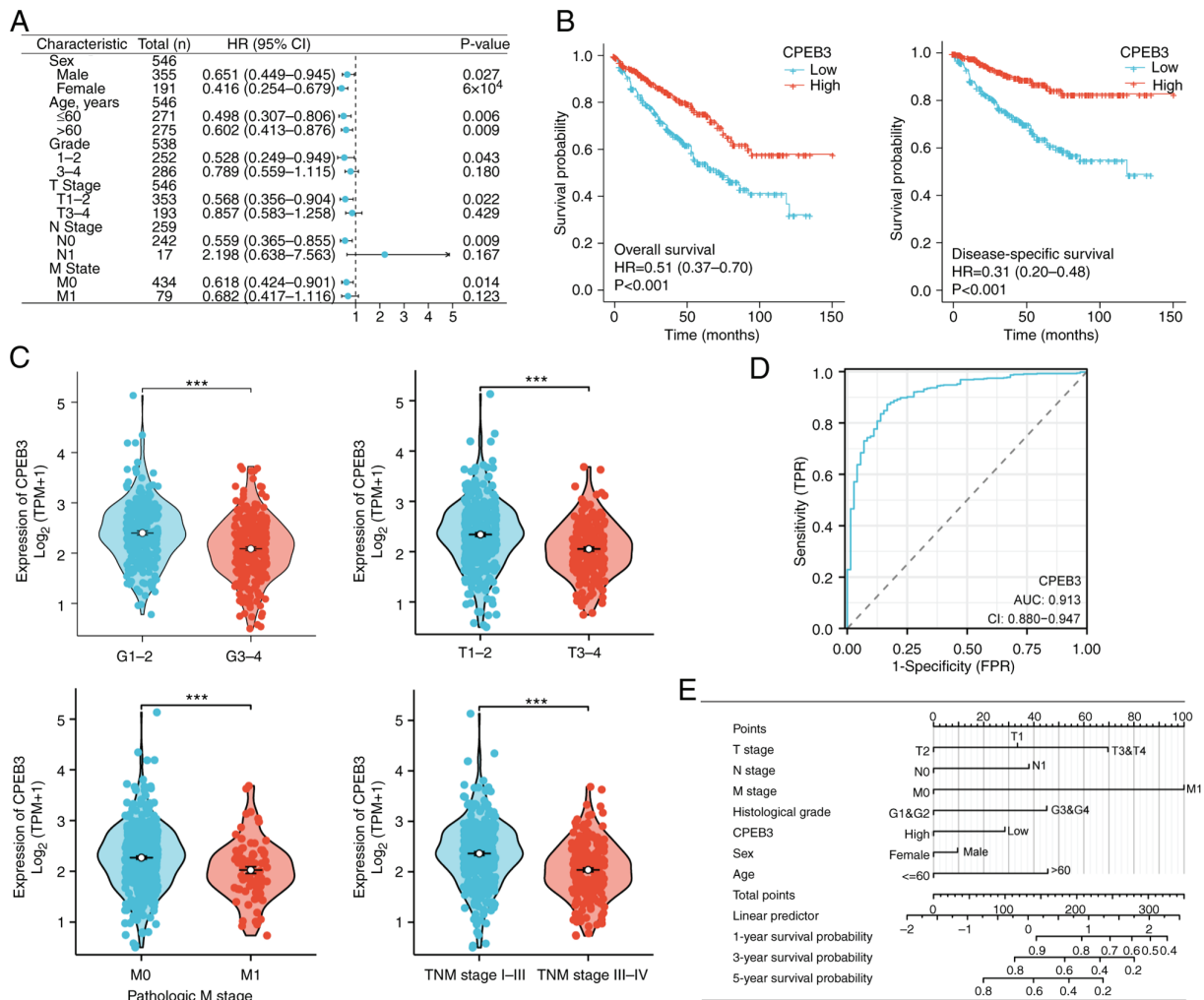


Figure 6. Clinical implications of CPEB3 in ccRCC. (A) Subgroup analysis of patients with ccRCC grouped by the expression of CPEB3. (B) Kaplan-Meier overall and disease-specific survival and DSS curves of ccRCC grouped by expression of CPEB3. (C) Associations between CPEB3 expression and clinical features. (D) Receiver operating characteristic curve of CPEB3 in ccRCC diagnosis. (E) Nomogram model includes clinical factors (T, N and M stages, histological grades, sex and age) and CPEB3 expression levels to predict the 1-, 3- and 5-year survival rates of patients with ccRCC. ***P<0.001. CPEB3, cytoplasmic polyadenylation element-binding protein 3; ccRCC, clear cell renal cell carcinoma; TPR, true positive rate; FPR, false positive rate; AUC, area under the curve.

direction for future research on CPEB3. Further experiments are required to confirm the functions of CPEB3 and its use as a novel biomarker and therapeutic target in ccRCC.

The present study demonstrated the prognostic and diagnostic value of CPEB3 in ccRCC. The expression of CPEB3 in ccRCC tissues was significantly lower than in normal tissue and its methylation level was higher. This indicated that CPEB3 may act as a tumor suppressor. CPEB3 may potentially serve as a favorable prognostic biomarker in ccRCC and patients with high CPEB3 expression are likely to have better outcomes. In addition, numerous types of infiltrating immune cell, particularly Tregs, were correlated with CPEB3 expression levels, suggesting that CPEB3 may affect TME and anti-tumor responses. Additional experimental and clinical studies are required to confirm these findings.

Acknowledgements

The authors would like to thank Mrs Fan Fan (Guangzhou Lupeng Pharmaceutical Co., Ltd. Guangzhou, Guangdong, China) for project management.

Funding

No funding was received.

Availability of data and materials

The data generated in the present study may be requested from the corresponding author.

Authors' contributions

HH and PO conceived and supervised the study, analyzed data and wrote and revised the manuscript. HH, PO, XS and WO designed the experiments. HH, PO, XS and WO performed experiments. HH and PO confirm the authenticity of all the raw data. All authors have read and approved the final manuscript.

Ethics approval and consent to participate

The Clinical Research Ethics Committee of Outdo BioTech granted ethical approval for the study of the tissue microarrays

(approval no. SHYJS-CP-1707003). Patient consent was obtained from all participants for participation in the study for use of their tissue.

Patient consent for publication

Not applicable.

Competing interests

The authors declare that they have no competing interests.

References

- Sung H, Ferlay J, Siegel RL, Laversanne M, Soerjomataram I, Jemal A and Bray F: Global cancer statistics 2020: GLOBOCAN estimates of incidence and mortality worldwide for 36 cancers in 185 countries. *CA Cancer J Clin* 71: 209-249, 2021.
- Leibovich BC, Lohse CM, Crispin PL, Boorjian SA, Thompson RH, Blute ML and Cheville JC: Histological subtype is an independent predictor of outcome for patients with renal cell carcinoma. *J Urol* 183: 1309-1315, 2010.
- Cella D, Motzer RJ, Suarez C, Blum SI, Ejzykowicz F, Hamilton M, Wallace JF, Simsek B, Zhang J, Ivanescu C, *et al*: Patient-reported outcomes with first-line nivolumab plus cabozantinib versus sunitinib in patients with advanced renal cell carcinoma treated in CheckMate 9ER: an open-label, randomised, phase 3 trial. *Lancet Oncol* 23: 292-303, 2022.
- Motzer R, Alekseev B, Rha SY, Porta C, Eto M, Powles T, Grünwald V, Hutson TE, Kopyltsov E, Méndez-Vidal MJ, *et al*: Lenvatinib plus pembrolizumab or everolimus for advanced renal cell carcinoma. *N Engl J Med* 384: 1289-1300, 2021.
- Choueiri TK, Powles T, Burotto M, Escudier B, Bourlon MT, Zurawski B, Oyervides Juárez VM, Hsieh JJ, Basso U, Shah AY, *et al*: Nivolumab plus cabozantinib versus sunitinib for advanced renal-cell carcinoma. *N Engl J Med* 384: 829-841, 2021.
- Powles T, Plimack ER, Soulières D, Waddell T, Stus V, Gafanov R, Nosov D, Pouliot F, Melichar B, Vynnychenko I, *et al*: Pembrolizumab plus axitinib versus sunitinib monotherapy as first-line treatment of advanced renal cell carcinoma (KEYNOTE-426): Extended follow-up from a randomised, open-label, phase 3 trial. *Lancet Oncol* 21: 1563-1573, 2020.
- Rini BI, Plimack ER, Stus V, Gafanov R, Hawkins R, Nosov D, Pouliot F, Alekseev B, Soulières D, Melichar B, *et al*: Pembrolizumab plus axitinib versus sunitinib for advanced renal-cell carcinoma. *N Engl J Med* 380: 1116-1127, 2019.
- Motzer RJ, Penkov K, Haanen J, Rini B, Albiges L, Campbell MT, Venugopal B, Kollmannsberger C, Negrier S, Uemura M, *et al*: Avelumab plus axitinib versus sunitinib for advanced renal-cell carcinoma. *N Engl J Med* 380: 1103-1115, 2019.
- Motzer RJ, Tannir NM, McDermott DF, Arén Frontera O, Melichar B, Choueiri TK, Plimack ER, Barthélémy P, Porta C, George S, *et al*: Nivolumab plus ipilimumab versus sunitinib in advanced renal-cell carcinoma. *N Engl J Med* 378: 1277-1290, 2018.
- Motzer RJ, Escudier B, McDermott DF, George S, Hammers HJ, Srinivas S, Tsykodi SS, Sosman JA, Procopio G, Plimack ER, *et al*: Nivolumab versus everolimus in advanced renal-cell carcinoma. *N Engl J Med* 373: 1803-1813, 2015.
- Choueiri TK, Tomczak P, Park SH, Venugopal B, Ferguson T, Chang YH, Hajek J, Symeonides SN, Lee JL, Sarwar N, *et al*: Adjuvant pembrolizumab after nephrectomy in renal-cell carcinoma. *N Engl J Med* 385: 683-694, 2021.
- Bi K, He MX, Bakouny Z, Kanodia A, Napolitano S, Wu J, Grimaldi G, Braun DA, Cuoco MS, Mayorga A, *et al*: Tumor and immune reprogramming during immunotherapy in advanced renal cell carcinoma. *Cancer Cell* 39: 649-661.e5, 2021.
- Wu F, Fan J, He Y, Xiong A, Yu J, Li Y, Zhang Y, Zhao W, Zhou F, Li W, *et al*: Single-cell profiling of tumor heterogeneity and the microenvironment in advanced non-small cell lung cancer. *Nat Commun* 12: 2540, 2021.
- Ma L, Hernandez MO, Zhao Y, Mehta M, Tran B, Kelly M, Rae Z, Hernandez JM, Davis JL, Martin SP, *et al*: Tumor cell biodiversity drives microenvironmental reprogramming in liver cancer. *Cancer Cell* 36: 418-430.e6, 2019.
- Barkley D, Moncada R, Pour M, Liberman DA, Dryg I, Werba G, Wang W, Baron M, Rao A, Xia B, *et al*: Cancer cell states recur across tumor types and form specific interactions with the tumor microenvironment. *Nat Genet* 54: 1192-1201, 2022.
- Nakamura K and Smyth MJ: Myeloid immunosuppression and immune checkpoints in the tumor microenvironment. *Cell Mol Immunol* 17: 1-12, 2020.
- Kumagai S, Koyama S, Itahashi K, Tanegashima T, Lin YT, Togashi Y, Kamada T, Irie T, Okumura G, Kono H, *et al*: Lactic acid promotes PD-1 expression in regulatory T cells in highly glycolytic tumor microenvironments. *Cancer Cell* 40: 201-218.e9, 2022.
- Naser R, Fakhoury I, El-Fouani A, Abi-Habib R and El-Sibai M: Role of the tumor microenvironment in cancer hallmarks and targeted therapy (review). *Int J Oncol* 62: 23, 2023.
- Josefowicz SZ, Lu LF and Rudensky AY: Regulatory T cells: Mechanisms of differentiation and function. *Annu Rev Immunol* 30: 531-564, 2012.
- Khattry R, Cox T, Yasayko SA and Ramsdell F: Pillars article: An essential role for scurf in CD4+CD25+ T regulatory cells. *Nat. Immunol.* 2003. 4: 337-342. *J Immunol* 198: 993-998, 2017.
- Hori S, Nomura T and Sakaguchi S: Control of regulatory T cell development by the transcription factor Foxp3. *Science* 299: 1057-1061, 2003.
- Fontenot JD, Gavin MA and Rudensky AY: Foxp3 programs the development and function of CD4+CD25+ regulatory T cells. *Nat Immunol* 4: 330-336, 2003.
- Sakaguchi S, Sakaguchi N, Asano M, Itoh M and Toda M: Immunologic self-tolerance maintained by activated T cells expressing IL-2 receptor alpha-chains (CD25). Breakdown of a single mechanism of self-tolerance causes various autoimmune diseases. *J Immunol* 155: 1151-1164, 1995.
- Tada Y, Togashi Y, Kotani D, Kuwata T, Sato E, Kawazoe A, Doi T, Wada H, Nishikawa H and Shitara K: Targeting VEGFR2 with Ramucirumab strongly impacts effector/activated regulatory T cells and CD8+ T cells in the tumor microenvironment. *J Immunother Cancer* 6: 106, 2018.
- Togashi Y and Nishikawa H: Regulatory T cells: Molecular and cellular basis for immunoregulation. *Curr Top Microbiol Immunol* 410: 3-27, 2017.
- Saito T, Nishikawa H, Wada H, Nagano Y, Sugiyama D, Atarashi K, Maeda Y, Hamaguchi M, Ohkura N, Sato E, *et al*: Two FOXP3(+)/CD4(+) T cell subpopulations distinctly control the prognosis of colorectal cancers. *Nat Med* 22: 679-684, 2016.
- Mendez R, Barnard D and Richter JD: Differential mRNA translation and meiotic progression require Cdc2-mediated CPEB destruction. *EMBO J* 21: 1833-1844, 2002.
- Chen J, Li L, Liu TY, Fu HF, Lai YH, Lei X, Xu JF, Yu JS, Xia YJ, Zhang TH, *et al*: CPEB3 suppresses gastric cancer progression by inhibiting ADAR1-mediated RNA editing via localizing ADAR1 mRNA to P bodies. *Oncogene* 41: 4591-4605, 2022.
- Cheng J, Ma H, Yan M, Zhang Z and Xing W: Circ_0007624 suppresses the development of esophageal squamous cell carcinoma via targeting miR-224-5p/CPEB3 to inactivate the EGFR/PI3K/AKT signaling. *Cell Signal* 99: 110448, 2022.
- Zhong Q, Fang Y, Lai Q, Wang S, He C, Li A, Liu S and Yan Q: CPEB3 inhibits epithelial-mesenchymal transition by disrupting the crosstalk between colorectal cancer cells and tumor-associated macrophages via IL-6R/STAT3 signaling. *J Exp Clin Cancer Res* 39: 132, 2020.
- Goldman MJ, Craft B, Hastie M, Repečka K, McDade F, Kamath A, Banerjee A, Luo Y, Rogers D, Brooks AN, *et al*: Visualizing and interpreting cancer genomics data via the Xena platform. *Nat Biotechnol* 38: 675-678, 2020.
- Vivian J, Rao AA, Nothhaft FA, Ketchum C, Armstrong J, Novak A, Pfeil J, Narkizian J, Deran AD, Musselman-Brown A, *et al*: Toil enables reproducible, open source, big biomedical data analyses. *Nat Biotechnol* 35: 314-316, 2017.
- Cancer Genome Atlas Research Network; Weinstein JN, Collisson EA, Mills GB, Shaw KR, Ozenberger BA, Ellrott K, Shmulevich I, Sander C and Stuart JM: The cancer genome atlas pan-cancer analysis project. *Nat Genet* 45: 1113-1120, 2013.
- GTEX Consortium: Human genomics. The genotype-tissue expression (GTEx) pilot analysis: Multitissue gene regulation in humans. *Science* 348: 648-660, 2015.
- R Core Team. R: A Language and Environment for Statistical Computing. R Foundation for Statistical Computing, Vienna, Austria, 2019.

36. Chandrashekar DS, Karthikeyan SK, Korla PK, Patel H, Shovon AR, Athar M, Netto GJ, Qin ZS, Kumar S, Manne U, *et al*: UALCAN: An update to the integrated cancer data analysis platform. *Neoplasia* 25: 18-27, 2022.
37. Chandrashekar DS, Basha B, Balasubramanya SAH, Creighton CJ, Ponce-Rodriguez I, Chakravarthi BVSK and Varambally S: UALCAN: A portal for facilitating tumor subgroup gene expression and survival analyses. *Neoplasia* 19: 649-658, 2017.
38. Love MI, Huber W and Anders S: Moderated estimation of fold change and dispersion for RNA-seq data with DESeq2. *Genome Biol* 15: 550, 2014.
39. Villanueva RAM and Chen ZJ: ggplot2: Elegant graphics for data analysis (2nd ed.). *Meas: Inter Res Perspect* 17: 160-167, 2019.
40. Ashburner M, Ball CA, Blake JA, Botstein D, Butler H, Cherry JM, Davis AP, Dolinski K, Dwight SS, Eppig JT, *et al*: Gene ontology: Tool for the unification of biology. The gene ontology consortium. *Nat Genet* 25: 25-29, 2000.
41. Gene Ontology Consortium; Aleksander SA, Balhoff J, Carbon S, Cherry JM, Drabkin HJ, Ebert D, Feuermann M, Gaudet P, Harris NL, *et al*: The gene ontology knowledgebase in 2023. *Genetics* 224: iyad031, 2023.
42. Yu G, Wang LG, Han Y and He QY: clusterProfiler: An R package for comparing biological themes among gene clusters. *OMICS* 16: 284-287, 2012.
43. Walter W, Sánchez-Cabo F and Ricote M: GOplot: An R package for visually combining expression data with functional analysis. *Bioinformatics* 31: 2912-2914, 2015.
44. Subramanian A, Tamayo P, Mootha VK, Mukherjee S, Ebert BL, Gillette MA, Paulovich A, Pomeroy SL, Golub TR, Lander ES and Mesirov JP: Gene set enrichment analysis: A knowledge-based approach for interpreting genome-wide expression profiles. *Proc Natl Acad Sci USA* 102: 15545-15550, 2005.
45. Liberzon A, Birger C, Thorvaldsdóttir H, Ghandi M, Mesirov JP and Tamayo P: The molecular signatures database (MSigDB) hallmark gene set collection. *Cell Syst* 1: 417-425, 2015.
46. Bindea G, Mlecnik B, Tosolini M, Kirilovsky A, Waldner M, Obenauf AC, Angell H, Fredriksen T, Lafontaine L, Berger A, *et al*: Spatiotemporal dynamics of intratumoral immune cells reveal the immune landscape in human cancer. *Immunity* 39: 782-795, 2013.
47. Hänzelmann S, Castelo R and Guinney J: GSEA: Gene set variation analysis for microarray and RNA-seq data. *BMC Bioinformatics* 14: 7, 2013.
48. Charoentong P, Finotello F, Angelova M, Mayer C, Efremova M, Rieder D, Hackl H and Trajanoski Z: Pan-cancer immunogenomic analyses reveal genotype-immunophenotype relationships and predictors of response to checkpoint blockade. *Cell Rep* 18: 248-262, 2017.
49. Li T, Fu J, Zeng Z, Cohen D, Li J, Chen Q, Li B and Liu XS: TIMER2.0 for analysis of tumor-infiltrating immune cells. *Nucleic Acids Res* 48 (W1): W509-W514, 2020.
50. Therneau TM: A package for survival analysis in R. <https://CRAN.R-project.org/package=survival>
51. Robin X, Turck N, Hainard A, Tiberti N, Lisacek F, Sanchez JC and Müller M: pROC: An open-source package for R and S+ to analyze and compare ROC curves. *BMC Bioinformatics* 12: 77, 2011.
52. Amin MB, Edge SB, Greene FL, Byrd DR, Brookland RK, Washington MK, Gershenwald JE, Compton CC, Hess KR, Sullivan DC, *et al* (eds): AJCC cancer staging manual. 8th edition. New York: Springer, 2017.
53. Pablo C, Marcela G, Lía EA and María IA: Correlation between MVD and two prognostic factors: Fuhrman grade and tumoral size, in clear cell renal cell carcinoma. *J Cancer Sci Ther* 4: 313-316, 2012.
54. Kim SP, Alt AL, Weight CJ, Costello BA, Cheville JC, Lohse C and Leibovich BC: Independent validation of the 2010 American joint committee on cancer TNM classification for renal cell carcinoma: Results from a large, single institution cohort. *J Urol* 185: 2035-2039, 2011.
55. Klatte T, Patard JJ, Goel RH, Kleid MD, Guille F, Lobel B, Abbou CC, De La Taille A, Tostain J, Cindolo L, *et al*: Prognostic impact of tumor size on pT2 renal cell carcinoma: An international multicenter experience. *J Urol* 178: 35-40, 2007.
56. Ged Y, Markowski MC, Singla N and Rowe SP: The shifting treatment paradigm of metastatic renal cell carcinoma. *Nat Rev Urol* 19: 631-632, 2022.
57. No authors listed: New treatments emerge for RCC. *Cancer Discov* 11: OF10, 2021.
58. Zilionis R, Engblom C, Pfirschke C, Savova V, Zemmour D, Saaticioglu HD, Krishnan I, Maroni G, Meyerovitz CV, Kerwin CM, *et al*: Single-cell transcriptomics of human and mouse lung cancers reveals conserved myeloid populations across individuals and species. *Immunity* 50: 1317-1334.e10, 2019.
59. Rosenthal R, Cadieux EL, Salgado R, Bakir MA, Moore DA, Hiley CT, Lund T, Tanić M, Reading JL, Joshi K, *et al*: Neoantigen-directed immune escape in lung cancer evolution. *Nature* 567: 479-485, 2019.
60. McGranahan N and Swanton C: Cancer evolution constrained by the immune microenvironment. *Cell* 170: 825-827, 2017.
61. Vesely MD, Kershaw MH, Schreiber RD and Smyth MJ: Natural innate and adaptive immunity to cancer. *Annu Rev Immunol* 29: 235-271, 2011.
62. Schreiber RD, Old LJ and Smyth MJ: Cancer immunoediting: Integrating immunity's roles in cancer suppression and promotion. *Science* 331: 1565-1570, 2011.
63. Koebel CM, Vermi W, Swann JB, Zerafa N, Rodig SJ, Old LJ, Smyth MJ and Schreiber RD: Adaptive immunity maintains occult cancer in an equilibrium state. *Nature* 450: 903-907, 2007.
64. Wolchok JD, Chiarion-Sileni V, Gonzalez R, Grob JJ, Rutkowski P, Lao CD, Cowey CL, Schadendorf D, Wagstaff J, Dummer R, *et al*: Long-Term outcomes with nivolumab plus ipilimumab or nivolumab alone versus ipilimumab in patients with advanced melanoma. *J Clin Oncol* 40: 127-137, 2022.
65. Taylor MH, Betts CB, Maloney L, Nadler E, Algazi A, Guarino MJ, Nemunaitis J, Jimeno A, Patel P, Munugala Vadla V, *et al*: Safety and efficacy of pembrolizumab in combination with acalabrutinib in advanced head and neck squamous cell carcinoma: Phase 2 proof-of-concept study. *Clin Cancer Res* 28: 903-914, 2022.
66. Slomski A: Pembrolizumab boosts breast and cervical cancer survival. *JAMA* 326: 2001, 2021.
67. Ferris RL, Blumenschein G Jr, Fayette J, Guigay J, Colevas AD, Licitra L, Harrington K, Kasper S, Vokes EE, Even C, *et al*: Nivolumab for recurrent squamous-cell carcinoma of the head and neck. *N Engl J Med* 375: 1856-1867, 2016.
68. Brahmer J, Reckamp KL, Baas P, Crinò L, Eberhardt WE, Poddubskaya E, Antonia S, Pluzanska A, Vokes EE, Holgado E, *et al*: Nivolumab versus docetaxel in advanced squamous-cell non-small-cell lung cancer. *N Engl J Med* 373: 123-135, 2015.
69. Ugel S, Canè S, De Sanctis F and Bronte V: Monocytes in the tumor microenvironment. *Annu Rev Pathol* 16: 93-122, 2021.
70. Li C, Teixeira AF, Zhu HJ and Ten Dijke P: Cancer associated-fibroblast-derived exosomes in cancer progression. *Mol Cancer* 20: 154, 2021.
71. Cheng HS, Lee JXT, Wahli W and Tan NS: Exploiting vulnerabilities of cancer by targeting nuclear receptors of stromal cells in tumor microenvironment. *Mol Cancer* 18: 51, 2019.
72. Quail DF, Bowman RL, Akkari L, Quick ML, Schuhmacher AJ, Huse JT, Holland EC, Sutton JC and Joyce JA: The tumor microenvironment underlies acquired resistance to CSF-1R inhibition in gliomas. *Science* 352: aad3018, 2016.
73. De Henau O, Rausch M, Winkler D, Campesato LF, Liu C, Cymerman DH, Budhu S, Ghosh A, Pink M, Tchaicha J, *et al*: Overcoming resistance to checkpoint blockade therapy by targeting PI3Ky in myeloid cells. *Nature* 539: 443-447, 2016.
74. Quail DF and Joyce JA: Microenvironmental regulation of tumor progression and metastasis. *Nat Med* 19: 1423-1437, 2013.
75. Coussens LM, Zitvogel L and Palucka AK: Neutralizing tumor-promoting chronic inflammation: A magic bullet? *Science* 339: 286-291, 2013.
76. Mao X, Xu J, Wang W, Liang C, Hua J, Liu J, Zhang B, Meng Q, Yu X and Shi S: Crosstalk between cancer-associated fibroblasts and immune cells in the tumor microenvironment: New findings and future perspectives. *Mol Cancer* 20: 131, 2021.
77. Erez N, Truitt M, Olson P, Arron ST and Hanahan D: Cancer-associated fibroblasts are activated in incipient neoplasia to orchestrate tumor-promoting inflammation in an NF-kappaB-dependent manner. *Cancer Cell* 17: 135-147, 2010.
78. Gajewski TF, Schreiber H and Fu YX: Innate and adaptive immune cells in the tumor microenvironment. *Nat Immunol* 14: 1014-1022, 2013.
79. Wade RJ and Burdick JA: Engineering ECM signals into biomaterials. *Mater Today* 15: 454-459, 2012.
80. Baumeister SH, Freeman GJ, Dranoff G and Sharpe AH: Coinhibitory pathways in immunotherapy for cancer. *Annu Rev Immunol* 34: 539-573, 2016.
81. Masugi Y, Nishihara R, Hamada T, Song M, da Silva A, Kosumi K, Gu M, Shi Y, Li W, Liu L, *et al*: Tumor PDCD1LG2 (PD-L2) expression and the lymphocytic reaction to colorectal cancer. *Cancer Immunol Res* 5: 1046-1055, 2017.

82. Wolf Y, Anderson AC and Kuchroo VK: TIM3 comes of age as an inhibitory receptor. *Nat Rev Immunol* 20: 173-185, 2020.
83. Anderson AC, Joller N and Kuchroo VK: Lag-3, Tim-3, and TIGIT: Co-inhibitory receptors with specialized functions in immune regulation. *Immunity* 44: 989-1004, 2016.
84. Reschke R and Gajewski TF: CXCL9 and CXCL10 bring the heat to tumors. *Sci Immunol* 7: eabq6509, 2022.
85. Duhon R, Fesneau O, Samson KA, Frye AK, Beymer M, Rajamanickam V, Ross D, Tran E, Bernard B, Weinberg AD and Duhon T: PD-1 and ICOS coexpression identifies tumor-reactive CD4+ T cells in human solid tumors. *J Clin Invest* 132: e156821, 2022.
86. Yan C and Richmond A: Hiding in the dark: Pan-cancer characterization of expression and clinical relevance of CD40 to immune checkpoint blockade therapy. *Mol Cancer* 20: 146, 2021.
87. Sugiura D, Maruhashi T, Okazaki IM, Shimizu K, Maeda TK, Takemoto T and Okazaki T: Restriction of PD-1 function by cis-PD-L1/CD80 interactions is required for optimal T cell responses. *Science* 364: 558-566, 2019.
88. Chen L, Diao L, Yang Y, Yi X, Rodriguez BL, Li Y, Villalobos PA, Cascone T, Liu X, Tan L, *et al*: CD38-mediated immunosuppression as a mechanism of tumor cell escape from PD-1/PD-L1 blockade. *Cancer Discov* 8: 1156-1175, 2018.
89. Liu Y, Wang L, Predina J, Han R, Beier UH, Wang LC, Kapoor V, Bhatti TR, Akimova T, Singhal S, *et al*: Inhibition of p300 impairs Foxp3+ T regulatory cell function and promotes antitumor immunity. *Nat Med* 19: 1173-1177, 2013.
90. Grebinoski S, Zhang Q, Cillo AR, Manne S, Xiao H, Brunazzi EA, Tabib T, Cardello C, Lian CG, Murphy GF, *et al*: Autoreactive CD8+ T cells are restrained by an exhaustion-like program that is maintained by LAG3. *Nat Immunol* 23: 868-877, 2022.
91. Klepsch V, Hermann-Kleiter N, Do-Dinh P, Jakic B, Offermann A, Efremova M, Sopper S, Rieder D, Krogsdam A, Gamerith G, *et al*: Nuclear receptor NR2F6 inhibition potentiates responses to PD-L1/PD-1 cancer immune checkpoint blockade. *Nat Commun* 9: 1538, 2018.



Copyright © 2024 Hong et al. This work is licensed under a Creative Commons Attribution-NonCommercial-NoDerivatives 4.0 International (CC BY-NC-ND 4.0) License.